Predicting microbial relative growth in a mixed culture from growth curve data

Yoav Ram[1*], Eynat Dellus-Gur[1], Maayan Bibi[2],

Uri Obolski[1], Judith Berman[2], and Lilach Hadany[1]

August 3, 2016

[1] Dept. Molecular Biology and Ecology of Plants, Tel Aviv University, Tel Aviv 69978, Israel

[2] Dept. of Molecular Microbiology and Biotechnology, Tel Aviv University, Tel Aviv 69978, Israel

[*] Corresponding author: yoavram@post.tau.ac.il

Keywords: mathematical model, fitness, selection coefficient, experimental evolution, microbial evolution, software

Abstract

Fitness is not well estimated from growth curves of individual isolates in monoculture. Rather, competition experiments, which measure relative growth in mixed microbial cultures, must be performed to better infer relative fitness. However, competition experiments require unique genotypic or phenotypic markers, and thus are difficult to perform with isolates derived from a common ancestor or non-model organisms. Here we describe *Curveball*, a new computational approach for predicting relative growth of microbes in a mixed culture utilizing mono- and mixed culture growth curve data. We implemented *Curveball* in an open-source software package (http://curveball.yoavram.com) and validated the approach using growth curve and competition experiments with bacteria. *Curveball* provides a simpler and more cost-effective approach to predict relative growth and infer relative fitness. Furthermore, by integrating several growth phases into the fitness estimation, *Curveball* provides a holistic approach to fitness inference from growth curve data.

Growth curves are commonly used in microbiology, genetics, and evolutionary biology to estimate the fitness of individual microbial isolates. Growth curves describe the density of cell populations in liquid culture over a period of time and are usually acquired by measuring the optical density (OD) of one or more cell populations. The simplest way to infer fitness from growth curves is to estimate the growth rate during the exponential growth phase by inferring the slope of the log of the growth curve[1] (see example in Figure 1). Indeed, the growth rate is often used as a proxy of the selection coefficient, *s*, which is the standard measure of relative fitness in population genetics[2,3]. However, exponential growth rates do not capture the dynamics of other phases of a typical growth curve, such as the length of lag phase and the cell density at stationary phase[4] (Figure 1). Thus, it is not surprising that growth rates are often poor estimators of relative fitness[5,6].

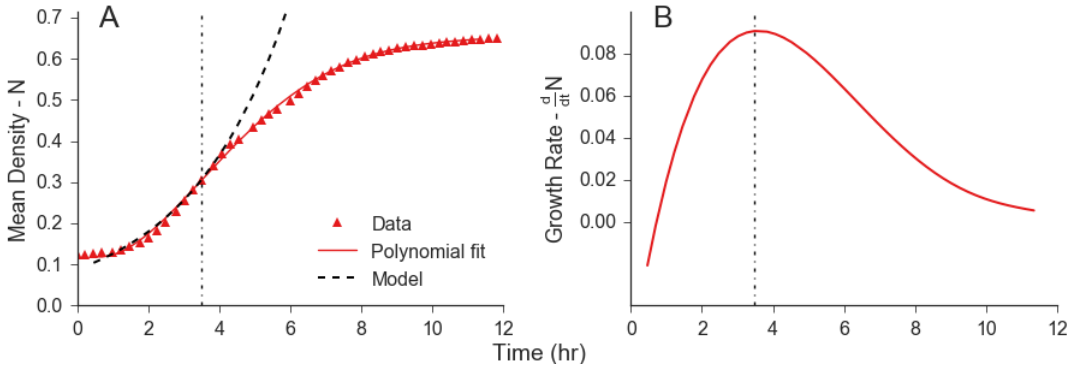

Figure 1. Fitting an exponential model to growth curve data. The growth rate is calculated as the derivative of a polynomial function fitted to the mean of the data $N(t)$: the time point of maximum growth rate t_{max} is found; 5 time points surrounding t_{max} are taken; a line of the form $b+at$ is fitted to the log of the mean of the data $log(N(t))$ at these time points; the intercept b and the slope a are interpreted as the initial density $N_0=e^b$ and the growth rate $r=a$ in an exponential growth model $N(t)=N_0e^{rt}$. **(A)** The red markers represent $N(t)$ the mean density in 22 growth curves. The solid red line represents the fitted polynomial. The dashed black line represents the exponential model N_0e^{rt} fitted to the data, with $N_0=0.058$ and $r=0.27$. The dotted vertical line denotes t_{max}, the time of max growth rate. **(B)** The red solid curve shows dN/dt, the derivative of the mean density (calculated as the derivative of the fitted polynomial). The dotted vertical line denotes t_{max}, the time of max growth rate. Data in this figure corresponds to the red growth curves from Figure 2A.

Evolutionary biologists use competition experiments to infer relative fitness in a manner that accounts for all growth phases[7]. In pairwise competition experiments, two strains are grown together in a mixed culture: a reference strain and a strain of interest. The frequency of each strain in the mixed culture is measured during the course of the experiment using specific markers[7] such as the expression of drug resistance markers on colony counts, fluorescent markers monitored by flow cytometry[8] or by deep sequencing read counts[9,10]. The selection coefficient of the

strains of interest can then be estimated from changes in their frequencies during the competition experiments. These methods can infer relative fitness with high precision[8], as they directly estimate fitness from changes in isolate frequencies over time. However, competition experiments are more laborious and expensive than monoculture growth curve experiments, requiring the development of genetic or phenotypic assays (see Concepción-Acevedo et al.[5] and references therein). Moreover, competition experiments are often impractical in non-model organisms. Therefore, many investigators prefer to use proxies of fitness such as growth rates.

Even when competition experiments are a plausible approach (for example, in microbial lineages with established markers[7]), methods for interpreting and understanding how differences in growth contribute to differences in fitness are lacking. Such differences have a crucial impact on our understanding of microbial fitness and the composition of microbial populations and communities.

Here we present *Curveball*, a new computational approach implemented in an open-source software package (http://curveball.yoavram.com). *Curveball* provides a predictive and descriptive framework for estimating growth parameters from growth dynamics, predicting relative growth in mixed cultures, and inferring relative fitness.

Results

Curveball consists of three stages: (a) fitting growth models to monoculture growth curve data, (b) fitting competition models to mixed culture growth curve data and using the estimated growth and competition parameters to predict relative growth in a mixed culture, and (c) inferring relative fitness from the predicted relative growth. The following experimental setting was used to test this approach.

a. Monoculture growth

In each experiment, two *Escherichia coli* strains, each labeled with a green or red fluorescent protein (GFP or RFP), were propagated in a monoculture and in a mixed culture, and the cell density was measured for each strain for at least 7 hours (Figure 2).

Growth model

The Baranyi-Roberts model[11] is used to model growth composed of several phases: lag phase, exponential phase, deceleration phase, and stationary phase[1]. The model assumes that growth rate accelerates as cells adjust to new growth conditions, then decelerates as resources become scarce, and finally halts when resources are depleted. The model is described by the following ordinary differential equation [see eqs. 1c, 3a, and 5a in[11]]:

$$\frac{dN}{dt} = r \cdot \alpha(t) \cdot N\left(1 - \left(\frac{N}{K}\right)^{\nu}\right) \quad [1]$$

where t is time, $N = N(t)$ is the population density at time t, r is the specific growth rate in low density, K is the maximum density, ν is a deceleration parameter, and $\alpha(t)$ is the adjustment function. For a derivation of eq. 1 and further details, see Supporting text 1.

The adjustment function $\alpha(t) = \frac{q_0}{q_0 + e^{-mt}}$ describes the fraction of the population that has adjusted to the new growth conditions by time t ($\alpha(t) \leq 1$). Typically, an overnight liquid culture of microorganisms that has reached stationary phase is diluted into fresh media. Following dilution, cells enter lag phase until they adjust to the new growth conditions. We chose the specific adjustment function suggested by Baranyi and Roberts[11], which is both computationally convenient and biologically interpretable: q_0 characterizes the physiological state of the initial population, and m is the rate at which the physiological state adjusts to the new growth conditions.

The Baranyi-Roberts differential equation (eq. 1) has a closed form solution:

$$N(t) = \frac{K}{\left[1 - \left(1 - \left(\frac{K}{N_0}\right)^{\nu}\right)e^{-r\,\nu A(t)}\right]^{1/\nu}} \quad [2]$$

where $N_0 = N(0)$ is the initial population density. For a derivation of eq. 2 from eq. 1, see Supporting text 1.

Model fitting

We estimated the growth model parameters by fitting the model (eq. 2) to the monoculture growth curve data of each strain. The best fit is shown in Figure 2D-F (see Table S1 for the estimated growth parameters). From this model fit we also estimate the maximum specific growth rate $\left(\max\left(\frac{1}{N}\cdot\frac{dN}{dt}\right)\right)$, the minimal specific doubling time, and the lag duration (Table 1). The strains differ in their growth parameters; for example, in experiment A (Figure 2A,D), the red strain grows 40% faster than the green strain, has 23% higher maximum density, and a 60% shorter lag phase.

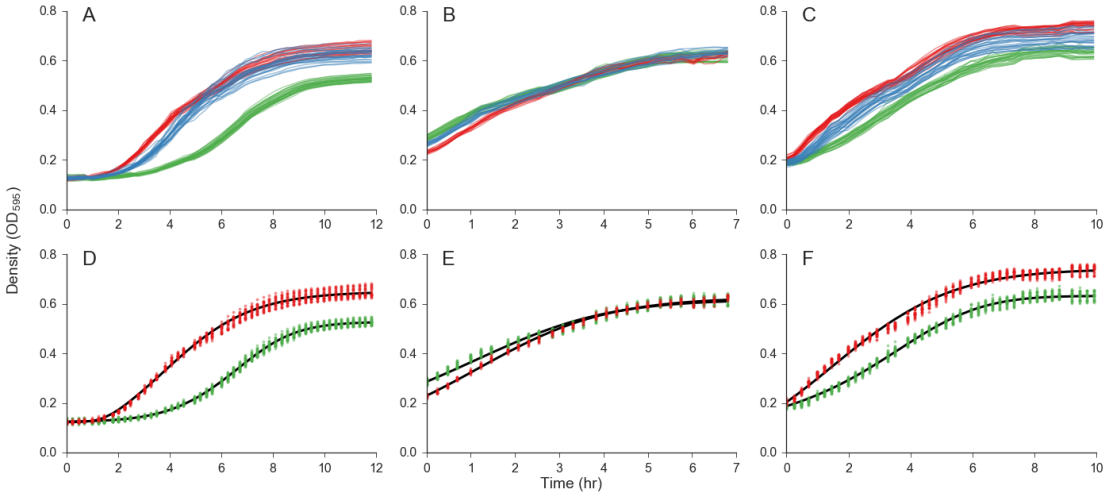

Figure 2. Fitting the growth model to growth curve data from three experiments with *E. coli*. (A-C) The top panels show the optical density (OD) of two strains growing in a monoculture (green lines for GFP labeled strain; red lines for RFP labeled strains) and a mixed culture (blue lines). Each of 30+ experimental replicates is represented by a separate line. **(D-F)** The bottom panels show the best model fit (solid black lines) for the growth curve data (markers, data corresponds to the curves in the top panels) of two strains (green and red) growing in monoculture. **(A,D)** Strain DH5α labeled with GFP, strain TG1 labeled with RFP. Experiment started by diluting stationary phase bacteria into fresh media, yielding a lag phase culture in which lag phase is longer for the green strain. **(B,E)** Strain DH5α labeled with GFP, strain TG1 labeled with RFP. Bacteria were pre-grown in fresh media for 4 hours before the experiment and then diluted into fresh media, such that there is no observable lag phase. **(C,F)** Strain JM109 labeled with GFP and, strain K12 MG1655-Δfnr labeled with RFP. Experimental conditions as described for (A,D).

	Experiment A		Experiment B		Experiment C	
Strain / ***Parameter***	**GFP**	**RFP**	**GFP**	**RFP**	**GFP**	**RFP**
Initial density (N_0)	0.125	0.124	0.286	0.23	0.188	0.204
Max density (K)	0.528 (0.525, 0.532)	0.650 (0.643, 0.658)	0.619 (0.612, 0.625)	0.627 (0.623, 0.631)	0.633 (0.627, 0.638)	0.741 (0.735, 0.746)
Max specific growth rate (μ)	0.268 (0.262, 0.274)	0.376 (0.371, 0.381)	0.256 (0.251, 0.261)	0.369 (0.354, 0.384)	0.228 (0.226, 0.23)	0.416 (0.392, 0.427)
Min doubling time (δ)	2.699 (2.636, 2.766)	1.843 (1.809, 1.88)	4.372 (4.276, 4.474)	2.450 (2.397, 2.506)	3.120 (3.087, 3.147)	2.075 (2.035, 2.124)
Lag duration (λ)	3.925 (3.822, 4.03)	1.578 (1.515, 1.639)	0.005 (0.002, 0.012)	0.014 (0.002, 0.029)	0.714 (0.684, 0.748)	0.045 (0.033, 0.081)

Table 1. Estimated growth parameters. 95% confidence intervals, calculated using bootstrap (1000 samples), are given in parentheses. Densities are in OD_{595}; growth rate in $hours^{-1}$, doubling time and lag duration in hours. See Table S2 for additional parameter estimates.

b. Mixed culture growth

Competition model

To model growth in a mixed culture, we assume that interactions between the strains are solely due to resource competition. We derived a new two-strain Lotka-Volterra competition model[12] based on resource consumption (see Supporting text 2):

$$\begin{cases} \frac{dN_1}{dt} = r_1\alpha_1(t)N_1\left(1 - \frac{N_1^{\nu_1}}{K_1^{\nu_1}} - \boldsymbol{a_2}\cdot\frac{N_2^{\nu_2}}{K_1^{\nu_1}}\right) & [3a] \\ \frac{dN_2}{dt} = r_2\alpha_2(t)N_2\left(1 - \boldsymbol{a_1}\cdot\frac{N_1^{\nu_1}}{K_2^{\nu_2}} - \frac{N_2^{\nu_2}}{K_2^{\nu_2}}\right) & [3b] \end{cases}$$

N_i is the density of strain $i = 1,2$ and $r_i, K_i, \nu_i, \alpha_i, q_{0,i}$, and m_i are the values of the corresponding parameters for strain i obtained from fitting the monoculture growth curve data. a_i are competition coefficients, the ratios between inter- and intra-strain competitive effects.

This competition model explicitly assumes that interactions between the strains are solely due to resource competition. Therefore, all interactions are described by the

158 deceleration of the growth rate of each strain in response to growth of the other strain.
159 Of note, each strain can have a different limiting resource and resource efficiency,
160 based on the maximum densities K_i and competition coefficients a_i determined for
161 each strain.

162 Eq. 3 is fitted to the growth curve of a mixed culture that includes both strains, in
163 which the combined OD of the strains is recorded over time (but not the frequency or
164 density of each individual strain). This fit is performed by minimizing the squared
165 differences between $N_1 + N_2$ (eq. 3) and the observed OD from the mixed culture and
166 yields estimates for the competition coefficients a_i (Figure 3A-C).

167 Using the estimated parameters, eq. 3 is solved by numerical integration, providing
168 a joint prediction for the densities $N_1(t)$ and $N_2(t)$. From the predicted densities, the
169 frequencies of each strain over time can be inferred: $f_i(t) = \frac{N_i(t)}{N_1(t)+N_2(t)}$.

170 **Prediction validation**

171 To test this method, we performed growth curve and competition experiments with
172 two different sets of *E. coli* strains marked with fluorescent proteins. In experiments A
173 and B we competed DH5α-GFP vs. TG1-RFP; in experiment C we competed JM109-
174 GFP with MG1655-Δfnr-RFP (see Figure 2A-C).

175 In each experiment, 32 replicate monocultures of the GFP strain, 30 replicate
176 monocultures of the RFP strain alone, and 32 replicate mixed cultures containing the
177 GFP and RFP strains together, were grown in a 96-well plate, under the same
178 experimental conditions. The optical density of each culture was measured every 15
179 minutes using an automatic plate reader. Samples were collected from the mixed
180 cultures every hour for the first 7-8 hours, and the relative frequencies of the two
181 strains were measured using flow cytometry (see
182 Materials and Methods).

183 Empirical competition results (green and red error bars), *Curveball* predictions
184 (green and red dashed lines), and exponential model prediction (dashed black lines;
185 see Figure 1 for details) for three different experiments are shown in Figure 3D-F.
186 *Curveball* performs well and clearly improves upon the exponential model for
187 predicting competition dynamics in a mixed culture.

188
189

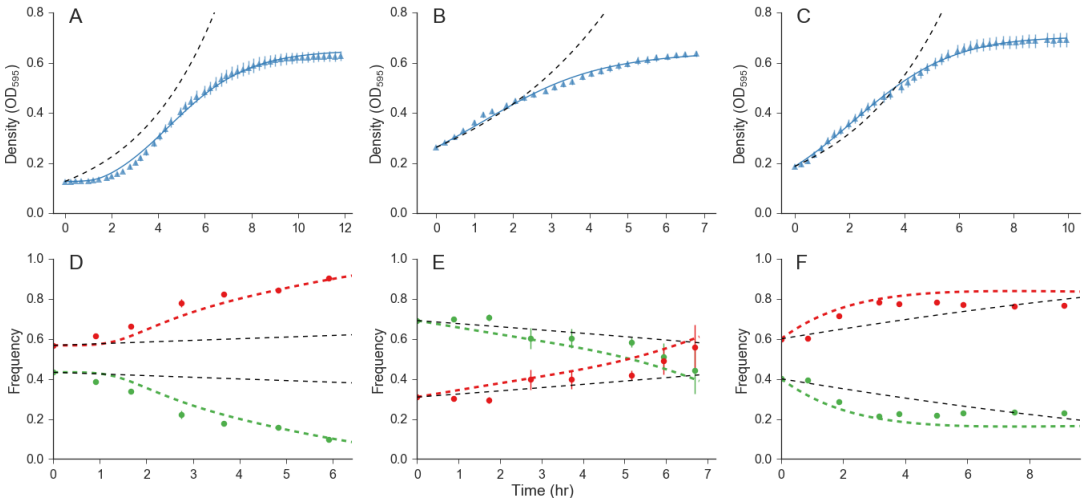

Figure 3. Predicting growth in a mixed culture. Growth of two *E. coli* strains competing for resources in a mixed culture. **(A-C)** Competition model fit (solid blue lines; eq. 3) for mixed culture growth curve data (triangles, data of blue lines in Figure 2A-C). Error bars show standard deviation from 30 replicates (extremely small in B); dashed black lines represent the exponential model prediction (see Figure 1). **(D-F)** Comparison of empirical (circles) and predicted (dashed lines; see Figure S3 for confidence intervals) strain frequencies in a mixed culture, corresponding to the growth curves in A-C. Green and red dashed lines show *Curveball* predictions; dashed black lines show exponential model predictions. Error bars show standard deviation (hardly seen in D and F). Root mean squared error of mixed culture fit (solid blue line to blue triangles): A, 0.011; B, 0.01; C, 0.008. Estimated competition coefficients: D, a_1=10, a_2=0.77; E, a_1=3.7, a_2=1.9; F, a_1=0.31, a_2=0.56. Inferred mean selection coefficients: D, 0.011; E, 0.01; F, 0.021.

c. Fitness inference

The best way to infer the relative fitness of two strains is to perform pairwise competition experiments[7]: growing both strains in a mixed culture and measuring the change in their frequencies over time. Using *Curveball*, pairwise competitions can be predicted by simply measuring the optical density during growth in mono- and mixed cultures, without directly measuring strain frequencies.

Relative fitness (given by 1+s,where s is the *selection coefficient* of the strain of interest) can be estimated from pairwise competition results using[3]:

$$s(t) = \frac{d}{dt}\log\left(\frac{N_2(t)}{N_1(t)}\right), \quad [4]$$

where $N_1(t)$ and $N_2(t)$ are the frequencies or densities of the strains and t is time. Using *Curveball*, we inferred the average selection coefficient of the red strain based upon eq. 4 applied to the predicted densities of the strains (Figure 3D-F): s=0.011, 0.01, and 0.021 in experiments A, B, and C, respectively.

Discussion

We developed *Curveball*, a new computational approach to predict relative growth in a mixed culture from growth curves of mono- and mixed cultures, without measuring frequencies of single isolates within the mixed culture. We tested and validated this new approach, which performed far better than the model commonly used in the literature. *Curveball* only assumes that the assayed strains grow in accordance with the growth and competition models: namely, that growth only depends on resource availability. Therefore, this approach can be applied to data from a variety of organisms, experiments, and conditions.

We have released an open-source software package which implements *Curveball* (http://curveball.yoavram.com). This software is written in Python[13] and includes a user interface that does not require prior knowledge in programming. It is free and open, such that additional data formats, growth and competition models, and other analyses can be added by the community to extend its utility.

Growth curve experiments, in which only optical density is measured, require much less effort and resources than pairwise competition experiments, in which the cell frequency or count of each strain must be determined[5,7,8,14]. Current approaches to estimating fitness from growth curves mostly use the growth rate or the maximum

population density as a proxy for fitness. However, the growth rate and other proxies for fitness based on a single growth parameter cannot capture the full scope of effects that contribute to differences in overall fitness[15].

In contrast, *Curveball* integrates several growth phases into the fitness estimation, allowing a more holistic approach to fitness inference from growth curve data and providing information on the specific growth traits that contribute to differences in fitness. We hope that *Curveball* will improve and ideally standardize the way fitness is estimated from growth curves, thereby improving communication between empirical and theoretical evolutionary biologists and ecologists.

Conclusions

We developed and tested a new method to analyze growth curve data, and applied it to predict growth of individual strains within a mixed culture and to infer their relative fitness. The method improves fitness estimation from growth curve data, has a clear biological interpretation, and can be used to predict and interpret growth in a mixed culture and competition experiments.

Materials and Methods

Strains and plasmids. *Escherichia coli* strains used were DH5α (Berman lab, Tel-Aviv University), TG1 (Ron lab, Tel-Aviv University), JM109 (Nir lab, Tel-Aviv University), and K12 MG1655-Δfnr (Ron lab, Tel-Aviv University). Plasmids containing a GFP or RFP gene and genes conferring resistance to kanamycin (Kan^R) and chloramphenicol (Cap^R) (Milo lab, Weizmann Institute of Science[16]). All experiments were performed in LB media (5 g/L Bacto yeast extract (BD, 212750), 10 g/L Bacto Tryptone (BD, 211705), 10 g/L NaCl (Bio-Lab, 190305), DDW 1 L) with 30 µg/mL kanamycin (Caisson Labs, K003) and 34 µg/mL chloramphenicol (Duchefa Biochemie, C0113). Green or red fluorescence of each strain was confirmed by fluorescence microscopy (Nikon Eclipe Ti, Figure S1).

Growth and competition experiments. All experiments were performed at 30°C. Strains were inoculated into 3 ml LB+Cap+Kan and grown overnight with shaking. Saturated overnight cultures were diluted into fresh media so that the initial OD was detectable above the OD of media alone (1:1-1:20 dilution rate). In experiments that

avoided a lag phase, cultures were pre-grown until the exponential growth phase was reached as determined by OD measurements (usually 4-6 h). Cells were then inoculated into 100 µL LB+Cap+Kan in a 96-well flat-bottom microplate (Costar):

- 32 wells contained a monoculture of the GFP-labeled strain
- 30 wells contained a monoculture of the RFP-labeled strain
- 32 wells containing a mixed culture of both GFP- and RFP-labeled strains
- 2 wells contained only growth medium

The cultures were grown in an automatic microplate reader (Tecan infinite F200 Pro), shaking at 886.9 RPM, until they reached stationary phase. OD_{595} readings were taken every 15 minutes with continuous shaking between readings.

Samples were collected from the incubated microplate at the beginning of the experiment and once an hour for 6-8 hours: 1-10 µL were removed from 4 wells (different wells for each sample), and diluted into cold PBS buffer (DPBS with calcium and magnesium; Biological Industries, 02-020-1). These samples were analyzed with a fluorescent cell sorter (Miltenyi Biotec MACSQuant VYB) with GFP detected using the 488nm/520(50)nm FITC laser and RFP detected with the 561nm/615(20)nm dsRed laser. Samples were diluted further to eliminate "double" event (events detected as both "green" and "red" due to high cell density) and noise in the cell sorter[8].

Fluorescent cell sorter output data was analyzed using R[17] with the *flowPeaks* package that implements an unsupervised flow cytometry clustering algorithm[18].

Data analysis. Growth curve data were analyzed using *Curveball*, a new open-source software written in Python[13] that implements the approach presented in this manuscript. The software includes both a programmatic interface (API) and a command line interface (CLI), and therefore does not require programming skills. The source code makes use of several Python packages: NumPy[19], SciPy[20], Matplotlib[21], Pandas[22], Seaborn[23], LMFIT[24], Scikit-learn[25], and SymPy[26].

Model fitting. To fit the growth and competition models to the growth curve data we use the *leastsq* non-linear curve fitting procedure[20,24]. We then calculate the Bayesian Information Criteria (BIC) of several nested models, defined by fixing some of the parameters (see Supporting text 1, Figure S2, and Table S1). BIC is given by:

$$BIC = n \cdot \log\left(\frac{\sum_{i=1}^{n}\left(N(t_i)-\widehat{N}(t_i)\right)^2}{n}\right) + k \cdot \log n,$$

where k is the number model parameters, n is the number of data points, t_i are the time points, $N(t_i)$ is the optical density at time point t_i, and $\widehat{N}(t_i)$ is the expected density at time point t_i according to the model. We selected the model with the lowest BIC[27,28].

Data availability. Data deposited on *figshare* (doi:10.6084/m9.figshare.3485984).

Code availability. Source code will be available upon publication at https://github.com/yoavram/curveball ; an installation guide, tutorial, and documentation will be available upon publication at http://curveball.yoavram.com.

Figure reproduction. Data was analyzed and figures were produced using a Jupyter Notebook[29] that will be available as a supporting file.

Acknowledgments

We thank Y. Pilpel, D. Hizi, I. Françoise, I. Frumkin, O. Dahan, A. Yona, T. Pupko, A. Eldar, I. Ben-Zion, E. Even-Tov, H. Acar, T. Pupko, and E. Rosenberg, for helpful discussions and comments, and L. Zelcbuch, N. Wertheimer, A. Rosenberg, A. Zisman, F. Yang, E. Shtifman Segal, I. Melamed-Havin, and R. Yaari for sharing materials and experimental advice. This research has been supported in part by the Israel Science Foundation 1568/13 (LH) and 340/13 (JB), the Minerva Center for Lab Evolution (LH), Manna Center Program for Food Safety & Security (YR), the Israeli Ministry of Science & Technology (YR), TAU Global Research and Training Fellowship in Medical and Life Science and the Naomi Foundation (MB), and the European Research Council (FP7/2007-2013)/ERC grant 340087 (JB).

Author contributions

All authors designed the experiments, analyzed data, discussed the results and edited the manuscript. Y.R. and L.H. developed the model and wrote the manuscript. U.O. advised on statistical analysis. Y.R. wrote the source code. Y.R., E.D.G. and M.B. performed the experiments. M.B. performed fluorescent microscopy. J.B. advised and gave support to all experiments. L.H. supervised all the work.

References

1. Hall, B. G., Acar, H., Nandipati, A. & Barlow, M. Growth rates made easy. *Mol. Biol. Evol.* **31,** 232–238 (2014).

2. Crow, J. F. & Kimura, M. *An introduction to population genetics theory*. (Burgess Pub. Co., 1970).

3. Chevin, L.-M. On measuring selection in experimental evolution. *Biol. Lett.* **7,** 210–3 (2011).

4. Wahl, L. M. & Zhu, A. D. Survival probability of beneficial mutations in bacterial batch culture. *Genetics* **200,** 309–20 (2015).

5. Concepción-Acevedo, J., Weiss, H. N., Chaudhry, W. N. & Levin, B. R. Malthusian Parameters as Estimators of the Fitness of Microbes: A Cautionary Tale about the Low Side of High Throughput. *PLoS One* **10,** e0126915 (2015).

6. Durão, P., Trindade, S., Sousa, A. & Gordo, I. Multiple Resistance at No Cost: Rifampicin and Streptomycin a Dangerous Liaison in the Spread of Antibiotic Resistance. *Mol. Biol. Evol.* msv143 (2015). doi:10.1093/molbev/msv143

7. Wiser, M. J. & Lenski, R. E. A Comparison of Methods to Measure Fitness in *Escherichia coli*. *PLoS One* **10,** e0126210 (2015).

8. Gallet, R., Cooper, T. F., Elena, S. F. & Lenormand, T. Measuring selection coefficients below 10^{-3}: method, questions, and prospects. *Genetics* **190,** 175–86 (2012).

9. Bank, C., Hietpas, R. T., Wong, A., Bolon, D. N. A. & Jensen, J. D. A Bayesian MCMC Approach To Assess the Complete Distribution of Fitness Effects of New Mutations: Uncovering the Potential for Adaptive Walks in Challenging Environments. *Genetics* **196,** 1–35 (2014).

10. Levy, S. F. *et al.* Quantitative evolutionary dynamics using high-resolution lineage tracking. *Nature* **519,** 181–186 (2015).

11. Baranyi, J. & Roberts, T. A. A dynamic approach to predicting bacterial growth in food. *Int. J. Food Microbiol.* **23,** 277–294 (1994).

12. Murray, J. D. *Mathematical Biology: I. An Introduction*. (Springer, 2002).

13. Van Rossum, G. & others. Python Programming Language. in *USENIX Annual*

Technical Conference (2007).

14. Hegreness, M., Shoresh, N., Hartl, D. L. & Kishony, R. An equivalence principle for the incorporation of favorable mutations in asexual populations. *Science (80-.).* **311,** 1615–7 (2006).

15. Bell, G. Experimental genomics of fitness in yeast. *Proc. R. Soc. B Biol. Sci.* **277,** 1459–1467 (2010).

16. Zelcbuch, L. *et al.* Spanning high-dimensional expression space using ribosome-binding site combinatorics. *Nucleic Acids Res.* **41,** e98–e98 (2013).

17. R Development Core Team. R: A Language and Environment for Statistical Computing. (2012).

18. Ge, Y. & Sealfon, S. C. flowPeaks: a fast unsupervised clustering for flow cytometry data via K-means and density peak finding. *Bioinformatics* **28,** 2052–2058 (2012).

19. van der Walt, S., Colbert, S. C. & Varoquaux, G. The NumPy Array: A Structure for Efficient Numerical Computation. *Comput. Sci. Eng.* **13,** 22–30 (2011).

20. Jones, E., Oliphant, T., Peterson, P. & others. SciPy: Open source scientific tools for Python. (2001). Available at: http://www.scipy.org/.

21. Hunter, J. D. Matplotlib: A 2D Graphics Environment. *Comput. Sci. Eng.* **9,** 90–95 (2007).

22. McKinney, W. Data Structures for Statistical Computing in Python. in *Proceedings of the 9th Python in Science Conference* (eds. van der Walt, S. & Millman, J.) 51–56 (2010).

23. Waskom, M. *et al.* seaborn: v0.7.0 (January 2016). (2016). doi:10.5281/zenodo.45133

24. Newville, M., Ingargiola, A., Stensitzki, T. & Allen, D. B. LMFIT: Non-Linear Least-Square Minimization and Curve-Fitting for Python. (2014). doi:10.5281/zenodo.11813

25. Pedregosa, F. *et al.* Scikit-learn: Machine Learning in Python. *J. Mach. Learn. Res.* **12,** 2825–2830 (2011).

384 26. SymPy Development Team. SymPy: Python library for symbolic mathematics.
385 (2014).

386 27. Kass, R. & Raftery, A. Bayes Factors. *J. Am. Stat. Assoc.* 773–795 (1995).
387 doi:doi: 10.2307/2291091

388 28. Ward, E. J. A review and comparison of four commonly used Bayesian and
389 maximum likelihood model selection tools. *Ecol. Modell.* **211,** 1–10 (2008).

390 29. Perez, F. & Granger, B. E. IPython: A System for Interactive Scientific
391 Computing. *Comput. Sci. Eng.* **9,** 21–29 (2007).

392 30. Otto, S. P. & Day, T. *A biologist's guide to mathematical modeling in ecology*
393 *and evolution*. (Princeton University Press, 2007).

394 31. Gopalsamy, K. Convergence in a resource-based competition system. *Bull.*
395 *Math. Biol.* **48,** 681–699 (1986).

396 32. Dilao, R. & Domingos, T. A General Approach to the Modelling of Trophic
397 Chains. *Ecol. Modell.* **132,** 20 (1999).

398 33. Richards, F. J. A Flexible Growth Function for Empirical Use. *J. Exp. Bot.* **10,**
399 290–301 (1959).

400 34. Baranyi, J. Simple is good as long as it is enough. *Commentary* 391–394
401 (1997). doi:10.1006/fmic.1996.0080

402 35. Clark, F., Brook, B. W., Delean, S., Reşit Akçakaya, H. & Bradshaw, C. J. A.
403 The theta-logistic is unreliable for modelling most census data. *Methods Ecol.*
404 *Evol.* **1,** 253–262 (2010).

405 36. Gilpin, M. E. & Ayala, F. J. Global Models of Growth and Competition. *Proc.*
406 *Natl. Acad. Sci. U. S. A.* **70,** 3590–3593 (1973).

407 37. Verhulst, P.-F. Notice sur la loi que la population suit dans son accroissement.
408 Correspondance Mathématique et Physique Publiée par A. *Quetelet* **10,** 113–
409 121 (1838).

410

Supporting material

Supporting text 1: Monoculture model

We derive our growth models from a resource consumption perspective[30,31]. We denote by R, the density of a limiting resource and by N the density of the population cells, both in total mass per unit of volume.

We assume that the culture is well-mixed and homogeneous and that the resource is depleted by the growing population without being replenished. Therefore, the intake of resources occurs when cells meet resource via a mass action law with resource intake rate h. Once inside the cell, resources are converted to cell mass at a rate ϵ. Cell growth is assumed to be proportional to $R \cdot N$, whereas resource intake is proportional to a power of cell density, $R \cdot N^{\nu}$. We denote $Y := N^{\nu}$.

We can describe this process with differential equations for R and N:

$$\begin{cases} \frac{dR}{dt} = -hRN^{\nu} & \text{[A1a]} \\ \frac{dN}{dt} = \epsilon hRN \end{cases}, \quad \text{[A1b]}$$

These equations can be converted to equations in R and Y:

$$Y = N^{\nu} \Rightarrow$$

$$\frac{dY}{dt} = \nu N^{\nu-1}\frac{dN}{dt} =$$

$$\nu N^{\nu-1} \cdot \epsilon hRN = \nu\epsilon hRN^{\nu},$$

which yields:

$$\begin{cases} \frac{dR}{dt} = -hRY & \text{[A2a]} \\ \frac{dY}{dt} = \mu hRY \end{cases}. \quad \text{[A2b]}$$

with $\mu = \epsilon\nu$.

To solve this system, we use a conservation law approach by setting $M = \mu R + Y$[32]. We find that M is constant:

$$\frac{dM}{dt} = \mu\frac{dR}{dt} + \frac{dY}{dt} \equiv 0,$$

and so we can substitute $\mu R = M - Y$ in eq. A2b:

$$\frac{dY}{dt} = hY(M - Y) = hMY\left(1 - \frac{Y}{M}\right). \quad \text{[A3]}$$

Substituting again $N^{\nu} = Y, \frac{dY}{dt} = \nu N^{\nu-1}\frac{dN}{dt}$, and defining $K = M^{\frac{1}{\nu}}, r = \frac{h}{\nu}K^{\nu}$, we get

$$\frac{dN}{dt} = r \cdot N \cdot \left(1 - \left(\frac{N}{K}\right)^{\nu}\right), \qquad [A4]$$

which is the Richards differential equation[33], with the maximum population density K and the specific growth rate in low density r: to the best of our knowledge this the first derivation of the Richards differential equation from a resource consumption perspective.

We solve eq. A4 via eq. A3, which is a logistic equation and therefore has a known solution. Setting the initial cell density $N(0) = N_0$:

$$N(t) = \frac{K}{\left(1-\left(1-\left(\frac{K}{N_0}\right)^{\nu}\right)e^{-r\nu t}\right)^{\frac{1}{\nu}}}.$$

Eq. A4 is an autonomous differential equation (dN/dt doesn't depend on t). To include a lag phase, Baranyi and Roberts[11] suggested to add an adjustment function $\alpha(t)$, which makes the equation non-autonomous (dependent on t):

$$\frac{dN}{dt} = r \cdot \alpha(t) \cdot N \cdot \left(1 - \left(\frac{N}{K}\right)^{\nu}\right). \qquad [A5]$$

Baranyi and Roberts suggested a Michaelis-Menten type of function $\alpha(t) = \frac{q_0}{q_0+e^{-mt}}$ [34], which has two parameters: q_0 is the initial physiological state of the population, and m is rate at which the physiological state adjusts to growth conditions. Integrating $\alpha(t)$ gives

$$A(t) := \int_0^t \alpha(s)ds = \int_0^t \frac{q_0}{q_0+e^{-ms}}ds = t + \frac{1}{m}\log\left(\frac{e^{-mt}+q_0}{1+q_0}\right).$$

Therefore, integrating eq. A5 produces eq. 2 in the main text.

The term $1-(N/K)^{\nu}$ is used to describe the deceleration in the growth of the population as it approaches the maximum density K. When $\nu = 1$, the deceleration is the same as in the standard logistic model $\left(\frac{dN}{dt} = r \cdot N \cdot \left(1 - \frac{N}{K}\right)\right)$ and the density at the time of the maximum growth rate $\left(\frac{d^2N}{dt^2}(t) = 0\right)$ is half the maximum density, $\frac{K}{2}$. When $\nu > 1$ or $1 > \nu$, the deceleration is slower or faster, respectively, and the density at the time of the maximum growth rate is $K/(1+\nu)^{1/\nu}$ (Richards 1959, substituting $\mathrm{W} = \mathrm{N}, \mathrm{A} = \mathrm{K}, \mathrm{m} = \nu + 1, \mathrm{k} = \mathrm{r} \cdot \nu$).

We use six forms of the Baranyi-Roberts model (Figure S2, Table S1). The full model is described by eq. 2 and has six parameters. A five parameter form of the model assumes $\nu = 1$, as in the standard logistic model, but still incorporates the adjustment function $\alpha(t)$ and therefore includes a lag phase. Another five parameter

461 form has both rate parameters set to the same value ($m = r$), which was suggested to
462 make the fitting procedure more stable[34,35]. A four parameter form has both of the
463 previous constraints, setting $m = r$ and $\nu = 1$[34]. Another four parameter form of the
464 model has no lag phase, with $1/m = 0 \Rightarrow \alpha(t) \equiv 1$, which yields the Richards
465 model[33], also called the θ-logistic model[36], or the generalized logistic model. This
466 form of the model is useful in cases where there is no observed lag phase: either
467 because the population adjusts very rapidly or because it is already adjusted prior to
468 the growth experiment, possibly by pre-growing it in fresh media before the beginning
469 of the experiment. The last form is the standard logistic model, in which $\nu = 1$ and
470 $1/m = 0$.

471 ## Supporting text 2: Mixed culture model

472 We now consider the case in which two species or strains grow in the same culture,
473 competing for a single limiting resource, similarly to eq. A1:

$$\begin{cases} \frac{dR}{dt} = -h_1 R N_1^{\nu_1} - h_2 R N_2^{\nu_2} & [B1a] \\ \frac{dN_1}{dt} = \epsilon_1 h_1 R N_1 & [B1b] \\ \frac{dN_2}{dt} = \epsilon_2 h_2 R N_2 & [B1c] \end{cases}$$

474 We define $Y_i = N_i^{\nu_i}$, and $M_i = \epsilon_i \nu_i R + Y_i + \frac{\epsilon_i \nu_i}{\epsilon_j \nu_j} Y_j$ (where *j* is 1 when *i* is 2 and
475 vice versa) to find that $\frac{dM_i}{dt} \equiv 0$ and M_i is constant. We then substitute $\epsilon_i \nu_i R = M_i -$
476 $Y_i - \frac{\epsilon_i \nu_i}{\epsilon_j \nu_j} Y_j$ into the differential equations for $\frac{dY_i}{dt}$. Denoting $K_i = M_i^{\frac{1}{\nu_i}}$ and $r_i = \frac{h_i}{\nu_i} K_i^{\nu_i}$,
477 we get:

$$\begin{cases} \frac{dN_1}{dt} = r_1 N_1 \left(1 - \frac{N_1^{\nu_1}}{K_1^{\nu_1}} - a_2 \cdot \frac{N_2^{\nu_2}}{K_1^{\nu_1}}\right) & [B2a] \\ \frac{dN_2}{dt} = r_2 N_2 \left(1 - a_1 \cdot \frac{N_1^{\nu_1}}{K_2^{\nu_2}} - \frac{N_2^{\nu_2}}{K_2^{\nu_2}}\right), & [B2b] \end{cases}$$

478 where $a_j = \frac{\epsilon_i \nu_i}{\epsilon_j \nu_j}$.

479 We get a similar result if each strain is limited by a different resource that both
480 strains consume:
481

$$\begin{cases} \frac{dR_1}{dt} = -h_1 R_1 N_1^{\nu_1} - h_2 R_1 N_2^{\nu_2} & [B3a] \\ \frac{dR_2}{dt} = -h_1 R_2 N_1^{\nu_1} - h_2 R_2 N_2^{\nu_2} & [B3b] \\ \frac{dN_1}{dt} = \epsilon_1 h_1 R_1 N_1 & [B3c] \\ \frac{dN_2}{dt} = \epsilon_2 h_2 R_2 N_2 & [B3d] \end{cases}$$

Here, we notice first that $\frac{d}{dt}\log(R_1) = \frac{d}{dt}\log(R_2)$ and therefore $\rho = \frac{R_1}{R_2}$ is a constant. We then substitute $R_1 = R, R_2 = \rho R$ in eqs. B3a-d and continue as above. This only changes the definition of $a_j = \frac{\epsilon_i \nu_i}{\epsilon_j \nu_j}\rho$.

If the intake rates depend only on the resource:

$$\begin{cases} \frac{dR_1}{dt} = -h_1 R_1 N_1^{\nu_1} - h_1 R_1 N_2^{\nu_2} & [B4a] \\ \frac{dR_2}{dt} = -h_2 R_2 N_1^{\nu_1} - h_2 R_2 N_2^{\nu_2} & [B4b] \end{cases}$$

Then we define $H = h_1/h_2$ and $\rho = \frac{R_1}{R_2^H}$ and again continue as above.

Supporting figures

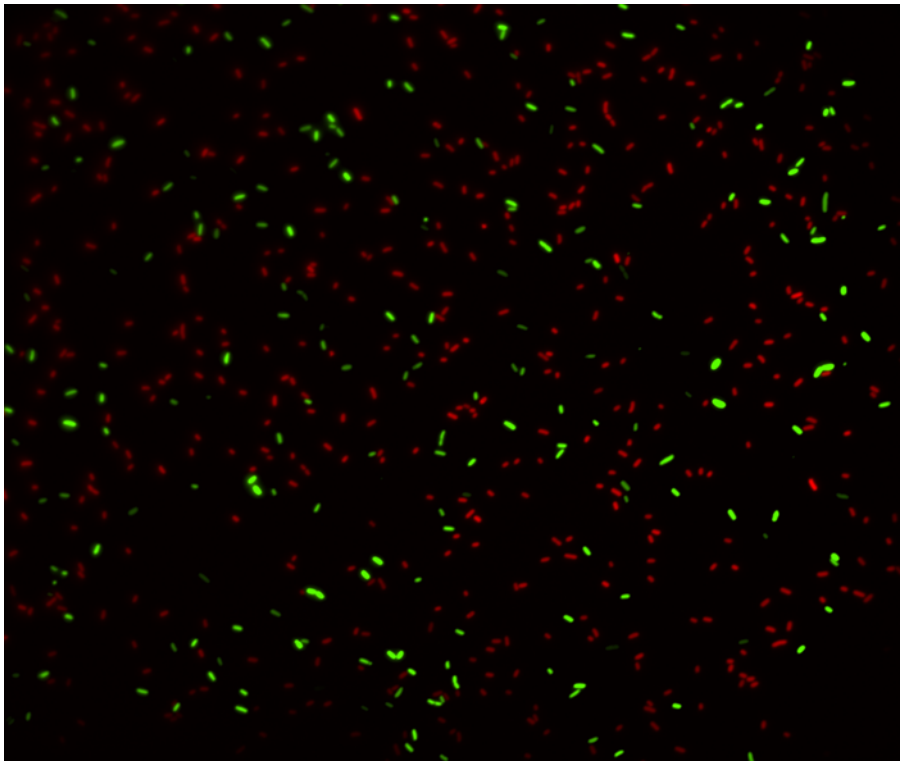

Figure S1. Fluorescence microscopy of *E. coli* strains carrying GFP or RFP. Image of a mixture of DH5α-GFP and TG1-RFP cells taken using a Nikon Eclipe Ti microscope.

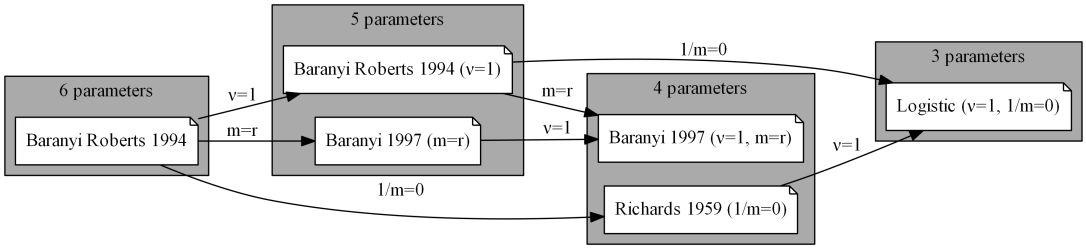

Figure S2. Growth models hierarchy. The Baranyi-Roberts model and five nested models defined by fixing one or two parameters. See Supporting text 1 and Table S1 for more details.

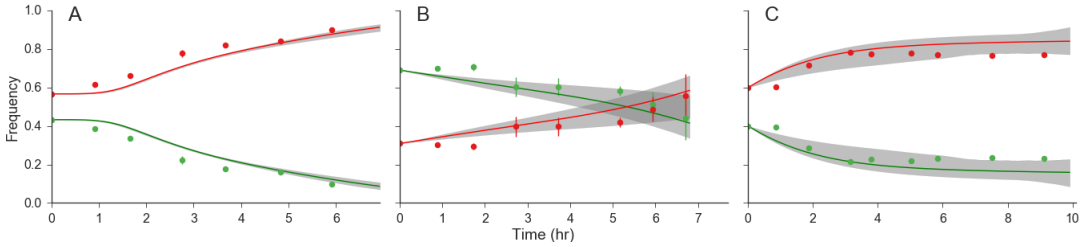

Figure S3. Mixed culture growth predictions with confidence intervals. The green and red lines correspond to the dashed green and red lines in Figure 3D-F, respectively. The gray area shows the 95% confidence interval, calculated using bootstrap (1000 samples).

Supporting tables

Model name	# Parameters	Free Parameters	Fixed Parameters	References
Baranyi Roberts 1994	6	N_0, K, r, ν, q_0, m	-	[11]
Baranyi 1997	5	N_0, K, r, ν, q_0	$m = r$	-
Baranyi Roberts 1994	5	N_0, K, r, q_0, m	$\nu = 1$	-
Richards 1959	4	N_0, K, r, ν	$\frac{1}{q_0} = \frac{1}{m} = 0$	[33]
Baranyi 1997	4	N_0, K, r, q_0	$\nu = 1$ $m = r$	[34]
Logistic	3	N_0, K, r	$\nu = 1$ $\frac{1}{q_0} = \frac{1}{m} = 0$	[37]

Table S1. Growth models. The table lists the growth models used for fitting growth curve data. All models are defined by eqs. 1 and 2, by fixing specific parameters. $\boldsymbol{N_0}$ is the initial population density; $\boldsymbol{K}$ is the maximum population density; $\boldsymbol{r}$ is the specific growth rate in low density; $\boldsymbol{\nu}$ is the surface to mass ratio; $\boldsymbol{q_0}$ is the initial physiological state; $\boldsymbol{m}$ is the physiological adjustment rate. Note that when $\boldsymbol{1/m = 0}$, the value of $\boldsymbol{q_0}$ is irrelevant. See also the hierarchy diagram in Figure S2 and a detailed discussion in Supporting text 1.

	Experiment A		Experiment B		Experiment C	
Strain	**GFP**	**RFP**	**GFP**	**RFP**	**GFP**	**RFP**
Parameter						
$\boldsymbol{N_0}$	0.125	0.124	0.286	0.23	0.188	0.204
$\boldsymbol{K}$	0.528	0.65	0.619	0.627	0.633	0.74
$\boldsymbol{r}$	0.376	0.587	0.304	0.484	8	8
$\boldsymbol{\nu}$	2.636	1*	2.484	1.491	1*	0.164
$\boldsymbol{q_0}$	0.032	0.008	-*	-*	0.039	0.393
$\boldsymbol{v}$	0.937	3.735	-*	-*	0.188	0.104

Table S2. Estimated parameters from growth model fitting. * denotes fixed parameters; - denotes invalid parameter values.